structure *c*-L (see Figure 1). Similar considerations hold for the complexes $L_nAg_n^+$ (**2** Figure 3, top).
[13] S. T. Howard, *J. Am. Chem. Soc.* **1996**, *118*, 10269; A. Göller, U.-W. Grummt, *Chem. Phys. Lett.* **2000**, *321*, 399.
[14] For examples of related intertwined structures of $[2 \times 2]$ grids, see: C. S. Campos-Fernández, R. Clérac, K. R. Dunbar, *Angew. Chem.* **1999**, *111*, 3685; *Angew. Chem. Int. Ed.* **1999**, *38*, 3477; X.-H. Bu, H. Morishita, K. Tanaka, K. Biradha, S. Furusho, M. Shionoya, *Chem. Commun.* **2000**, 971.
[15] P. N. W. Baxter, J.-M. Lehn, K. Rissanen, *Chem. Commun.* **1997**, 1323.
[16] Several attempts to obtain useful electrospray mass spectral data for the mixtures of $Ag^I$ complexes and for the final grid **1** were unfortunately fruitless, in contrast to studies of mixtures of related $Cu^I$ complexes.[15]
[17] These data involve a) mutual relaxation cross-peaks between the methyl groups of the three transoid ligands, and b) significant differences in $T_1$ relaxation times of the central pyridazine hydrogens in the transoid (2.1 s) and in the cisoid (1.3 s) ligands.
[18] J.-M. Lehn in *Supramolecular Science*: *Where It Is and Where It Is Going* (Eds.: R. Ungaro, E. Dalcanale), Kluwer, Amsterdam, **1999**, p. 287.
[19] a) As a first approximation, one may assume that free bipy and 9,10-phenanthroline (phen) are models for binding to a transoid and a cisoid site respectively in ligand L. Then, binding of one free ligand L (*all-trans*) and three $Ag^+$ ions to the $L_5Ag_6^+$ species *c*-**3** may be estimated to amount to a free energy of about 45 kcal mol$^{-1}$, corresponding to the formation of three mixed-ligand $Ag^+$(bipy,phen) complexes, which would each provide a binding free energy of $[Ag^+(bipy)_2/2 + Ag^+(phen)_2/2] = 10/2 + 20/2 = 15$ kcal mol$^{-1}$.[19c] Note that the difference between binding of $Ag^+$ to a single phen and a single bipy $(20\text{-}10)/2 = 5$ kcal mol$^{-1}$ should compare to a cisoid into transoid conversion that is, 6 – 8 kcal mol$^{-1}$;[12] b) we realize that this data "torturing" may already be going too far… Molecular-mechanics Universal-Force-Field calculations provide an energy difference of about 50 kcal mol$^{-1}$ between *c*-**3** and *t*-**3**; E. Ruiz, unpublished work. *Ab initio* calculations on different complexes have been undertaken; G. Corongiu, P. Nava, work in progress; c) this corresponds to complexation in acetonitrile: W. J. Peard, R. T. Pflaum, *J. Am. Chem. Soc.* **1958**, *80*, 1593.
[20] For a discussion of the enthalpic component in positive cooperativity brought in by structural tightening, see: C. T. Calderone, D. H. Williams, *J. Am. Chem. Soc.* **2001**, *123*, 6262.
[21] $\Delta\Delta G$ provides in principle a direct quantitative measure (when it can be accurately determined) of cooperativity: S. Forsén, S. Linse, *Trends Biochem. Sci.* **1995**, *20*, 495.
[22] I. Tinoco, Jr., K. Sauer, J. C. Wang, *Physical Chemistry*, Prentice-Hall, Upper Saddle River, **1995**, pp. 638 – 648.
[23] A. Pfeil, J.-M. Lehn, *J. Chem. Soc. Chem. Commun.* **1992**, 838; T. M. Garrett, U. Koert, J.-M. Lehn, *J. Phys. Org. Chem.* **1992**, *5*, 529. For another process see E. Leize, A. Van Dorsselaer, R. Krämer, J.-M. Lehn, *J. Chem. Soc. Chem. Commun.* **1993**, 990.
[24] S. Shinkai, M. Ikeda, A. Sugasaki, M. Takeuchi, *Acc. Chem. Res.* **2001**, *34*, 394, and references therein.
[25] E. Di Cera, *Chem. Rev.* **1998**, *98*, 1563.

# Electrochemical Modulation of Fluorophore Emission on a Nanostructured Gold Film**

Prashant V. Kamat,* Said Barazzouk, and Surat Hotchandani

Fluorophore-bound gold nanoparticles can serve as a probe in biological systems, provide basic understanding of molecular-level interactions of a surface-bound organic moiety,[1–4] and contribute to the development of biological tracers as well as optoelectronic devices.[5–8] In a fluorophore – gold nanoassembly the charge transfer interaction between the two components plays an important role as it dictates the pathways by which the excited state deactivates. For example, in the case of 1-aminomethylpyrene the transfer of lone-pair electrons to gold nanoparticles led to a fluorescence enhancement.[9] On the other hand, the fluorescence emission of a pyrenylthiol ((1-pyrenyl)-6-oxaheptanethiol) was quenched through charge transfer upon binding to the gold nanoparticles.[10]

Gold nanoparticles capped with organic molecules have a unique ability to retain the charge when subjected to an electric field. Their ability to display quantized charging has been demonstrated by Murray and coworkers.[6, 11] Control of charging of the gold nanocore thus becomes an important factor if one is interested in modulating the interaction between the gold nanocore and a surface-bound fluorophore. In order to systematically assess the effect of charging on the photochemistry of surface-bound molecules, we have conducted spectroelectrochemical measurements using nanostructured gold films that were functionalized with a pyrenylthiol and have succeeded in modulating the fluorescence using an externally applied electrochemical bias. The possibility of achieving electrochemical modulation of the fluorescence of a gold-surface-bound fluorophore opens up new avenues to design sensors, displays, and biological probes.

Earlier studies have shown that fluorophores bound to bulk metal surfaces are nonfluorescent.[1, 12–14] Both energy transfer and electron transfer processes are considered to be major deactivation pathways for the excited fluorophore on metal surfaces. Our recent study has shown the possibility of achieving a photoinduced electron transfer in colloidal suspensions of pyrenylthiol-functionalized gold nanoparti-

[*] Dr. P. V. Kamat, S. Barazzouk
Notre Dame Radiation Laboratory
Notre Dame, IN 46556-0579 (USA)
Fax: (+1) 574-631-8068
E-mail: pkamat@nd.edu
Dr. S. Hotchandani
Groupe de Recherche en Énergie et Information Biomoléculaires
Université du Québec à Trois-Rivières
Trois-Rivières, PQ, G9A 5H7 (Canada)

[**] We thank Mr. Binil I. Ipe and Dr. K. George Thomas of the Regional Research Laboratory, Trivandrum, India, for a sample of (1-pyrenyl)-6-oxaheptanethiol. The research described here was supported by the Office of Basic Energy Science of the Department of Energy. This is contribution no. NDRL 4354 from the Notre Dame Radiation Laboratory. S.B. and S.H. acknowledge support of the Natural Sciences and Engineering Research Council of Canada.

Supporting information for this article is available on the WWW under http://www.angewandte.org or from the author.

  0044-8249/02/11415-2888 $ 20.00+.50/0 

cles.[10] If indeed the gold particles act as electron acceptors, it should be possible to modulate the electron transfer quenching of the excited fluorophore by charging the gold nanoparticle at an electrode surface. The charging of organo-capped gold nanoparticles has been demonstrated by monitoring the shift of the plasmon band to lower energies.[15] However, the shift in the plasmon band was too small (5–9 nm) to resolve these charging effects. Surface-bound fluorophores, on the other hand, provide a new way to monitor the charging events.

In the present study, we have functionalized gold nanoparticles with two different thiols at the same time; one contained a fluorophore (pyrene) and the other a carboxylic acid residue. The latter (sulfanylpropionic acid) served to link the gold nanoparticles to the $TiO_2$ surface. The electrode preparation is illustrated in Scheme 1. A similar strategy of using difunctional surface modifiers to link different nanoparticles has been demonstrated earlier.[16–18] The presence of sulfanylpropionic acid also helps to distribute the pyrene moieties around the gold nanocore with minimal intermolecular interactions. Based on the concentration and particle size we estimate an average of about 20 pyrene moieties per gold nanoparticle.

Figure 1 shows the absorption spectra of an OTE/$TiO_2$ electrode before (b) and after (a) modification with pyrene-functionalized gold nanoparticles. Within minutes of insertion of the OTE/$TiO_2$ electrode into the THF solution containing the functionalized gold nanoparticles **1** we can observe changes in the electrode coloration. The transparent electrode quickly turns dark purple, thereby confirming the binding of the gold nanoparticles. The electrodes were repeatedly washed with THF to remove any unbound gold nanoparticles. The AFM image (see Figure 1 of the Supporting Information) reveals a highly porous morphology with particle domains of 100 nm diameter. The electrode shows a broad absorption in the visible region with a maximum around 530 nm. This absorption is characteristic of the surface plasmon band of gold nanoparticles and is possibly broadened because of their interaction with the $TiO_2$ film. Because of the strong absorbance of $TiO_2$ in the UV region, we could not further resolve the pyrene absorption bands.

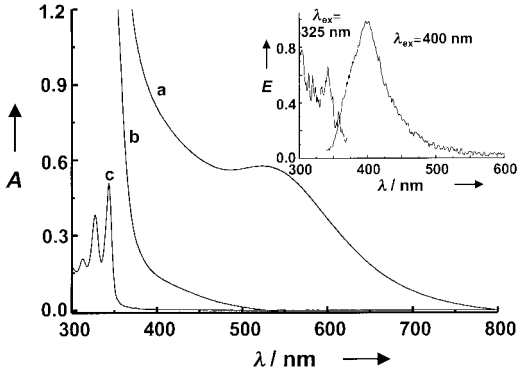


Figure 1. Absorption spectra of a) OTE/$TiO_2$/**1**, b) OTE/$TiO_2$, and c) (1-pyrenyl)-6-oxaheptanethiol in THF. The inset shows the excitation and emission spectra of the OTE/$TiO_2$/**1** electrode recorded at no applied electrochemical bias. The excitation and monitoring wavelengths for these two spectra were 325 nm and 400 nm, respectively.

In the inset of Figure 1 the excitation and emission spectra of the OTE/$TiO_2$/**1** electrode are shown. The electrode exhibits weak emission (monitoring wavelength $\lambda = 400$ nm) with a maximum around 395 nm. As discussed in our previous study,[10] most of the emission of surface-bound pyrene is quenched by the gold nanocore. Decreased singlet lifetime as well as formation of the oxidation product, pyrene radical cation, indicated the ability of gold nanoparticles to accept electrons from excited pyrene.[19]

The weak fluorescence seen in Figure 1 stems from pyrene moieties that do not undergo quenching on the gold surface. The excitation spectrum in the inset ($\lambda_{ex} = 325$ nm) shows the absorption response in the UV (corresponding to the absorption bands at 342, 320, and 314 nm), thereby confirming that the emission arises from surface-bound pyrene. (The front-face geometry as well as the low emission yield limited the resolution of the absorption bands in the excitation spectra.) Another interesting observation was the absence of excimer emission bands in the spectrum of **1** bound to a $TiO_2$ surface (inset of Figure 1). This contrasts with the observation in colloidal suspension in which we observed excimer emission arising from intermolecular interactions on the gold surface (see Figure 2 of the Supporting Information). The absence of pyrene excimer emission in the film suggests that the molecular movement of the excited-state pyrene moieties is significantly restricted when they are assembled on the $TiO_2$ surface.

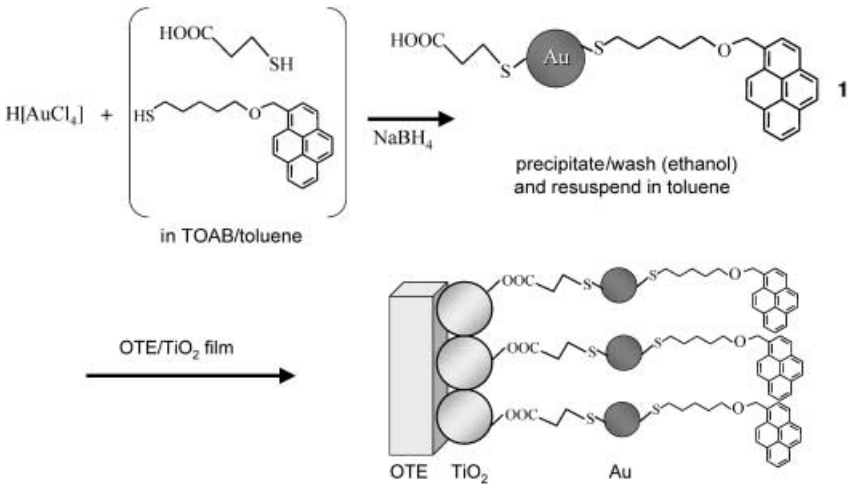


Scheme 1. Functionalization of gold nanoparticles with a pyrenylthiol and their binding to a nanostructured $TiO_2$ film. TOAB = tetraoctylammonium bromide, OTE = optically transparent electrode.

Spectroelectrochemical experiments were conducted using a thin-layer electrochemical cell in a spectrofluorimeter with front-face geometry. Figure 2 shows the emission spectra of OTE/$TiO_2$/**1** at different applied potentials. In a previous study we had shown that gold particles deposited on a nanostructured $TiO_2$ film permit the flow of electrons following Fermi level equili-

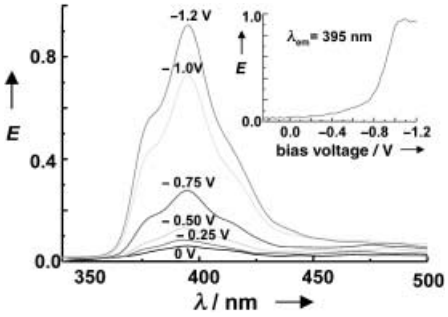


Figure 2. Emission spectra of OTE/$TiO_2$/**1** at different applied potentials using an excitation wavelength of 325 nm. The electrode was maintained at a set potential (0 to −1.2 V vs SCE, electrolyte: 0.1M tetrabutylammoniumperchlorate in acetonitrile) for 5 min before recording the individual emission spectrum. The inset shows the fluorescence response of OTE/$TiO_2$/**1** at 395 nm during the electrochemical scan.

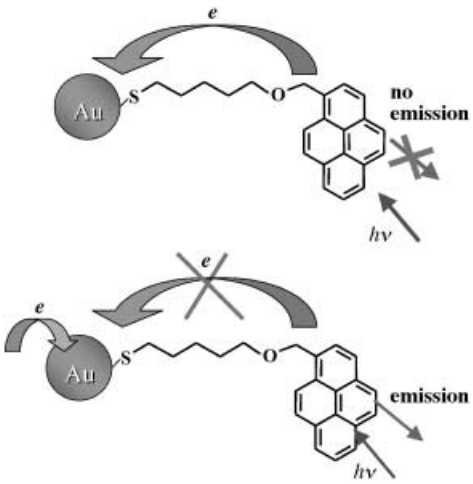


Scheme 2. Deactivation of excited surface-bound pyrene a) before and b) after charging the gold nanocore.

bration.[20] Moreover, the pyrene-modified electrodes can also exhibit sensitized photocurrent response when subjected to photoexcitation (Figure 3 of the Supporting Information). As we bias the electrode to negative potentials we observe an increase in the emission yield. It is important to note that the overall shape of the emission band essentially remains the same. This in turn suggests that the photoactive species that contribute to the emission remain unperturbed. As we bias the electrode to more negative potentials, the gold particles become charged and fewer pyrene moieties interact with the gold surface. At potentials around −1.2 V we completely suppress the interaction between the fluorophore and the gold nanocore, and we achieve saturation in the emission increase. We were able to restore more than 90% of the quenched emission by simply charging the gold nanoparticle with an externally applied electrochemical bias. The fluorescence response (at 395 nm) of OTE/$TiO_2$/**1** recorded during an electrochemical scan is shown in the inset of Figure 2. By controlling the applied electrochemical potential one can modulate the pyrene fluorescence at a desired level.

The fact that the spectral features of the pyrene emission hardly change during the sweep of the electrochemical potential suggests that the biasing of the electrode to negative potentials does not cause any pyrene desorption. This aspect was independently confirmed by testing the electrolyte solution from the cell for pyrene emission after the application of a negative bias. The absorption spectrum of the electrode recorded after the spectroelectrochemical experiments did not indicate any deterioration of the film. These results confirm that an externally applied electrochemical bias does not cause any desorption of the surface-bound fluorophore. Its role remains modulation of the excited state dynamics of the surface-bound pyrene.

Scheme 2 illustrates the excited state behavior of surface-bound pyrene in the absence and presence of an applied bias. We expect a majority of the surface-bound pyrene moieties to actively participate in the electron transfer quenching at 0 V or under no electrochemical bias. As we sweep the potential to more negative values, the gold nanocores become charged, thus shifting the quasi-Fermi level to a more negative potential. The quantized charging effects studied with organo-capped gold nanoparticles suggest that the potential shift amounts to about 0.1 V per accumulated electron.[11] Hence, the electron transfer from excited pyrene molecules to the gold nanocore experiences a barrier as we apply a negative electrochemical bias. Surface binding of pyrene to the gold surface through an amine group leads to a similar enhancement in the fluorescence yield.[9] Transfer of lone-pair electrons from the amine group to the gold nanocore resulted in the suppression of the intramolecular quenching process between amine and pyrene moieties.

Basic understanding of the photophysical properties of a surface-bound molecule is important to elucidate the charge transfer interactions as well as the microsurroundings near the metal nanocore. The possibility of electrochemically modulating the fluorescence of a fluorophore on a nanostructured gold electrode opens up new avenues to probe interfacial charge transfer processes. These fluorescence modulation studies also demonstrate the possibility of utilizing noble metal–fluorophore nanoassemblies for sensor and display applications.

### *Experimental Section*

The original procedure[21] for preparing gold colloids in an organic medium was modified. An aqueous solution of hydrogen tetrachloroaurate(III) hydrate (0.023 g, 0.06 mmol in 2 mL) was mixed with a solution of TOAB (0.1366 g, 0.25 mmol) in 5 mL toluene. The biphasic mixture was vigorously stirred until all the tetrachloroaurate was transferred into the organic layer. A solution of sulfanylpropionic acid (5 mg) and (1-pyrenyl)-6-oxaheptanethiol (3 mg) in 1 mL toluene was added to the gold solution (Au/S molar ratio 1:1). (The preparation of the pyrenylthiol was described earlier.[10]) After stirring for 2–3 min, a solution of sodium tetrahydroborate (0.1M) in water (2 mL) was added, and the mixture was stirred for 3 h. The organic layer was separated off and concentrated to 2.5 mL in a rotavap. After addition of ethanol (150 mL), the mixture was cooled to 273 K for 12 h and then in ice–salt mixture for 2–3 h to 255 K. The functionalized gold nanoparticles which settled at the bottom of the flask were filtered and washed with ethanol (5 × 250 mL). The dark brown powder composed of nanoparticles 2–3 nm diameter in size was redispersible in toluene and other organic solvent such as THF.

Colloidal $TiO_2$ was prepared by hydrolyzing titanium(IV) isopropoxide in water containing acetic acid. The OTEs were cut (1 × 5 cm) from a Pilkington TEC glass (glass plate coated with indium tin oxide). The OTE/$TiO_2$ electrodes were prepared by casting a thin film of colloidal $TiO_2$ on OTE plates and drying in air. Scanning electron micrographs show an

  0044-8249/02/11415-2890 $ 20.00+.50/0 

assembly of $TiO_2$ particles 20–30 nm diameter in size, that is of highly porous morphology. After annealing at 673 K for 1 h the electrodes were modified with pyrene-functionalized gold nanoparticles by immersing into a THF solution of the nanoparticles overnight. The electrodes were washed thoroughly with THF to remove any unbound gold nanoparticles. These electrodes are referred to as OTE/$TiO_2$/**1**.

Absorption spectra were recorded with a Shimadzu 3101 spectrophotometer, transmission electron micrographs (TEM) with a Hitachi H600 transmission electron microscope. For the spectroelectrochemical experiments a Princeton applied research model 175 galvanostat/potentiostat was used, details of which can be found elsewhere.[22] The fluorescence from the nanostructured gold film was monitored with an SLM S-8000 photon-counting spectrofluorimeter in a front-face geometry. The other components of the cell were a Pt counter electrode, a saturated calomel reference electrode (SCE) and acetonitrile containing 0.1M tetrabutylammonium perchlorate (TBAP) as electrolyte.

Received: December 27, 2001
Revised: May 6, 2002 [Z18441]

[1] O. V. Makarova, A. E. Ostafin, H. Miyoshi, J. R. Norris, D. Meisel, *J. Phys. Chem. B* **1999**, *103*, 9080.
[2] A. C. Templeton, W. P. Wuelfing, R. W. Murray, *Acc. Chem. Res.* **2000**, *33*, 27.
[3] A. N. Shipway, E. Katz, I. Willner, *PhysChemPhys* **2000**, *1*, 18.
[4] X. M. Zhao, Y. N. Xia, G. M. Whitesides, *J. Mater. Chem.* **1997**, *7*, 1069.
[5] J. J. Hickman, D. Ofer, P. E. Laibinis, G. M. Whitesides, M. S. Wrighton, *Science* **1991**, *252*, 688.
[6] S. Chen, R. S. Ingram, M. J. Hostetler, J. J. Pietron, R. W. Murray, T. G. Schaaff, J. T. Khoury, M. M. Alvarez, R. L. Whetten, *Science* **1998**, *280*, 2098.
[7] R. Elghanian, J. J. Storhoff, R. C. Mucic, R. L. Letsinger, C. A. Mirkin, *Science* **1997**, *277*, 1078.
[8] W. P. McConnell, J. P. Novak, L. C. Brousseau III, R. R. Fuierer, R. C. Tenent, D. L. Feldheim, *J. Phys. Chem. B* **2000**, *104*, 8925.
[9] K. G. Thomas, P. V. Kamat, *J. Am. Chem. Soc.* **2000**, *122*, 2655.
[10] B. I. Ipe, K. G. Thomas, S. Barazzouk, S. Hotchandani, P. V. Kamat, *J. Phys. Chem. B* **2002**, *106*, 18.
[11] S. Chen, R. W. Murray, *J. Phys. Chem. B* **1999**, *103*, 9996.
[12] P. Avouris, B. N. J. Persson, *J. Phys. Chem.* **1984**, *88*, 837.
[13] K. Saito, *J. Phys. Chem. B* **1999**, *103*, 6579.
[14] T. Pagnot, D. Barchiesi, G. Tribillon, *Appl. Phys. Lett.* **1999**, *75*, 4207.
[15] A. C. Templeton, J. J. Pietron, R. W. Murray, P. Mulvaney, *J. Phys. Chem. B* **2000**, *104*, 564.
[16] P. V. Kamat, M. de Lind, S. Hotchandani, *Isr. J. Chem.* **1993**, *33*, 47.
[17] D. Lawless, S. Kapoor, D. Meisel, *J. Phys. Chem.* **1995**, *99*, 10329.
[18] M. Brust, J. Fink, D. Bethell, D. J. Schiffrin, C. Kiely, *J. Chem. Soc. Chem. Commun.* **1995**, 1655.
[19] The oxidation potential of excited pyrene is around $-1.5$ V versus NHE, which thermodynamically favors transfer of electrons to gold nanoparticles ($E_F = 0.5$ V).
[20] V. Subramanian, E. Wolf, P. V. Kamat, *J. Phys. Chem. B* **2001**, *105*, 11439.
[21] M. Brust, M. Walker, D. Bethell, D. J. Schiffrin, R. Whyman, *J. Chem. Soc. Chem. Commun.* **1994**, 801.
[22] P. V. Kamat, I. Bedja, S. Hotchandani, L. K. Patterson, *J. Phys. Chem. B* **1996**, *100*, 4900.

# Valence-Ordering Structures and Magnetic Behavior of Metallic MMX Chain Compounds**

Minoru Mitsumi,* Kouhei Kitamura, Ayumi Morinaga, Yoshiki Ozawa, Mototada Kobayashi, Koshiro Toriumi,* Yasuhito Iso, Hiroshi Kitagawa, and Tadaoki Mitani

Recently, 1D halogen-bridged mixed-valence dinuclear metal complexes, so-called MMX chain compounds, have attracted significant attention as quasi-1D electronic systems characterized by strong electron–phonon, electron–electron, and magnetic interactions. Only two families of MMX chain compounds, namely $[\{A_4[Pt_2(pop)_4X]\cdot n H_2O\}_\infty]$ (pop = $P_2O_5H_2^{2-}$, A = Li, K, Cs, $NH_4$, X = Cl, Br, I)[1] and $[\{M_2(dta)_4I\}_\infty]$ (dta = $CH_3CS_2^-$, M = Ni, Pt)[2] have been reported. These compounds are 1D chain systems based on a mixed-valence dinuclear unit with a formal oxidation number of +2.5 and a metal–metal bond with a formal bond order of 1/2. An important feature of MMX chain compounds is the increase in internal degrees of freedom upon introducing a dinuclear unit in the mixed-valence state. This property enables a variety of electronic structures, represented by the extreme valence-ordering states shown in Figure 1. These valence-ordering structures would be classified based on the periodicity of the 1D chains as follows. The averaged valence (AV) and charge-polarization (CP) states, in which the periodicity of 1D chains is M-M-X-, correspond to a metallic state with an effective half-filled conduction band mainly composed of M–Md$\sigma$*–X$p_z$-hybridized orbitals or to the Mott–Hubbard semiconducting state. In contrast, the periodicity of 1D chains in the charge density wave (CDW) and alternate charge-polarization (ACP) states is doubled, and these electronic structures are regarded as Peierls and spin-Peierls states,[3] respectively.

Kitagawa et al. have reported that $[\{Pt_2(dta)_4I\}_\infty]$ exhibits metallic conducting behavior above 300 K in an AV state.[2d] On the results of a $^{129}$I Mössbauer spectroscopic study, the valence-ordering structure of this compound at temperatures

[*] Dr. M. Mitsumi, Prof. Dr. K. Toriumi, K. Kitamura, A. Morinaga, Prof. Dr. Y. Ozawa, Prof. Dr. M. Kobayashi
Department of Material Science
Himeji Institute of Technology
3-2-1 Kouto, Kamigori-cho, Hyogo 678-1297 (Japan)
Fax: (+81) 791-58-0155
E-mail: mitsumi@sci.himeji-tech.ac.jp, toriumi@sci.himeji-tech.ac.jp
Y. Iso, Prof. Dr. H. Kitagawa,[+] Prof. Dr. T. Mitani
Japan Advanced Institute of Science and Technology
Tatsunokuchi, Ishikawa 923-1292 (Japan)
[+] Current address: Department of Chemistry
University of Tsukuba
Tsukuba 305-8571 (Japan)

[**] This work was supported by a Grants-in-Aids for Scientific Research (10740307 and 09440232) and Priority Areas "Metal-Assembled Complexes" (11136244) from the Ministry of Education, Science, Sports and Culture, Japan. M.M. gratefully appreciates Prof. Dr. N. Sakai for use of the SQUID magnetometer. M = metal center, X = halogen.

Supporting information for this article is available on the WWW under http://www.angewandte.org or from the author.